Limited Bandwidth Recognition of Collective Behaviors in Bio-Inspired Swarms

Daniel S. Brown
AFRL Information Directorate
26 Electronic Parkway
Rome, NY 13441
daniel.brown.81@us.af.mil

Michael A. Goodrich
Department of Computer Science
Brigham Young University
Provo, UT 84602
mike@cs.byu.edu

ABSTRACT

Models of swarming and modes of controlling them are numerous; however, to date swarm researchers have mostly ignored a fundamental problem that impedes scalable human interaction with large bio-inspired robot swarms, namely, how do you know what the swarm is doing if you can't observe every agent in the collective? We examine swarm models that exhibit multiple collective motion patterns from the same parameters. These multiple emergent behaviors provide increased expressivity, but at the cost of uncertainty about the swarm's actual behavior. Because bandwidth and time constraints limit the number of agents that can be observed in a swarm, it is desirable to be able to recognize and monitor the collective behavior of a swarm through limited samples from a small subset of agents. We present a novel framework for classifying the collective behavior of a bio-inspired robot swarm using locally-based approximations of a swarm's global features. We apply this framework to two bio-inspired models of swarming that exhibit a flock and torus behavior and a swarm, torus, and flock behavior, respectively. We present both a formal metric of expressivity and a classifier that leverages local agent-level features to accurately recognize these collective swarm behaviors while sampling from only a small number of agents.

Categories and Subject Descriptors

I.2.11 [**Artificial Intelligence**]: Distributed Artificial Intelligence—*multiagent systems, mobile agents*

General Terms

Algorithms, Design, Experimentation, Performance

Keywords

Swarms and collective behaviors, behavior recognition, bio-inspired robotics, human-swarm interaction, self-organization

1. INTRODUCTION

Swarms have been hailed as the future of low cost multi-agent systems because of their inherent robustness, flexibility, and the power of obtaining complex behaviors from many simple local interactions [16]. Biologically-inspired robot swarms are typically characterized by a large number of agents with limited abilities and are ideally suited for accomplishing dangerous or uncertain tasks where communication is limited and agent failures are likely. In many situations, such as search and rescue, military operations, and space exploration, it is desirable to have a robust robot team that is amenable to human interaction. As these bio-inspired teams grow in size, bandwidth and time constraints make it increasingly difficult for a human to individually control and monitor every agent. Thus, there is a need for limited bandwidth methods to monitor and influence the collective behavior of a swarm. This is especially important because many swarm applications may involve contested or uncertain environments where maintaining communication with a large proportion of the swarm is unlikely.

Swarm models and control methods are numerous; however, most research has avoided the problem of recognizing the collective behavior of a swarm. We address this research gap by demonstrating a methodology for accurately detecting the emergent collective motion of a robot swarm using limited information from only a subset of the swarm.

The methodology we propose leverages the fact that collective behaviors are often fundamental attractors of multi-agent dynamic systems [19, 3, 10], and thus have distinct global structure. Because this global structure is a function of local behaviors, we use local samples of agent-level features to estimate the collective behavior of a swarm. Previous work by Kerman et al. [6] demonstrates a bio-inspired swarm model that exhibits two stable emergent behaviors: a flock and a torus. The work by Kerman et al. also shows the existence of what we term an *expressive region* in the parameter space, that allows multiple emergent behaviors from the same parameters. The existence of an expressive region affords switching between swarm behaviors on the fly by only influencing a subset of the swarm. Our work examines the problem of recognizing the collective behavior of a swarm that is operating in an expressive region, using information from only a subset of the swarm.

Using the model proposed by Kerman et al. [6], we show that classification between a flock and torus is possible with high accuracy simply by sampling a small number of agents and using a simple classifier. In fact, we demonstrate that because of the high degree of structure found in the collective behaviors of the swarm, these behaviors can be quickly and accurately classified even if agents are unable to perform self-localization. Using local information on perceived numbers of neighbors and angular velocity from a subset of

Appears in: *Alessio Lomuscio, Paul Scerri, Ana Bazzan, and Michael Huhns (eds.), Proceedings of the 13th International Conference on Autonomous Agents and Multiagent Systems (AAMAS 2014), May 5-9, 2014, Paris, France.*

agents, we demonstrate this concept using a simple naive Bayes classifier to accurately detect whether the swarm is moving as a torus or as a flock. We also examine a similar bio-inspired model proposed by Couzin et al. [3] that has three distinct collective behaviors: swarm, torus, and flock. We empirically show that this model also has an expressive region that allows both a flock and a torus behavior, and demonstrate that local observations can be used to recognize the collective behaviors in this swarm model.

2. RELATED WORK

Swarm models have been explored by many researchers in a wide variety of fields. These models are typically capable of either flocking [15, 21, 12] or cyclic behavior [8, 7], and in some cases can exhibit multiple group behaviors depending on the model parameters used [6, 3, 17]. However, to cause a swarm to switch between behaviors typically requires changing the model parameters. While much work in the swarm literature has investigated swarm behaviors and phase transitions between then [22], we know of little work, other than that by Kerman et al. [6], that has investigated models that produce multiple behaviors from the same parameters.

Strömbom [17] proposes an attraction-only swarm model and shows evidence of several regions in the parameter space that exhibit two different behaviors using the same model parameters; however, this model uses periodic boundary conditions and it is unclear whether these expressive regions persist if these boundary conditions are removed. Work by Nevai et al. explores the problem of how a honeybee colony evaluates the quality of a potential nest site [10]. They develop a dynamic model of the nest-site selection process and determine conditions under which the colony can switch between model equilibria. However, this work is for a group decision process, not a group formation control problem which is the focus of our research.

The work that is probably most similar to ours is the research in multi-agent activity recognition [18, 20, 14, 11]. However, our work differs from previous multi-agent activity recognition approaches in that we seek to identify the emergent behavior of a large collective by combining (a) observations of a few individuals with (b) knowledge of the attractor structures that describe these collective behaviors.

3. SWARM MODEL

The majority of our analysis and experiments focus on a model of swarming published by Kerman et al. [6]. The model consists of a set of N agents with the dynamics for agent i given by

$$\dot{x_i} = s \cdot \cos\theta_i,\ \dot{y_i} = s \cdot \sin\theta_i,\ \dot{\theta_i} = \omega_i, \qquad (1)$$

where $c_i(t) = [x_i(t), y_i(t)]^T \in \mathbb{R}^2$ is the agent's position at time t, $\theta_i \in [-\pi, \pi]$ is the agent's angular heading, s is the constant agent speed, and ω_i is the agent's angular velocity. The magnitude of ω_i is bounded by $\pi/2$. Thus, the agent dynamics match the Dubins curve model which is often used for actual UAV path planning and applies to many constant-speed, non-holonomic ground robots [5]. Similar to the Couzin model of biological swarms [3] and the Reynold model of synthetic agents [15], agents in this model react to neighbors within three different zones: repulsion, orientation, and attraction. An agent is repelled from neighbors within its repulsion zone of radius R_r, orients its heading with neighbors in its orientation zone of radius R_o, and is attracted to neighbors outside of its orientation zone. The angular velocity ω_i is determined by summing the desired direction vectors resulting from the repulsion, orientation, and attraction rules.

(a) torus (b) flock

Figure 1: Emergent swarm behaviors in Kerman's model. Straight lines represent agent headings.

Neighbors are chosen with a random neighbor model where, at each time step, agent i is visible to agent j according to a Bernoulli random variable with parameter $p_{ij}(t) = \min\left(1, 1/\|c_i(t) - c_j(t)\|_2\right)$. This method of choosing neighbors is similar to the random neighbor model used in [1] which replicated field observations of starlings and is relevant for actual robot systems which are noisy and where visibility and sensing are less likely with growing distance.

3.1 Emergent behaviors

This model has two emergent behaviors: a torus and a flock, shown in Figure 1. A torus has a relatively stationary group centroid, and either a clockwise or counterclockwise rotation. The torus behavior could potentially be used for perimeter monitoring, for a fixed-wing UAV loitering command, or to provide omni-directional sensing of a target. A flock has a moving centroid with all of the agents heading in the same general direction. The flock behavior is ideal for transporting the swarm quickly from one location to another and could be used for search or for tracking moving objects.

Previous work has shown that the torus and flock behaviors are actually fundamental attractors of the attraction and orientation dynamics of this model [6, 2]. Additionally, work in [6] determined parameter values that allow both group types to emerge. The percentage of trials that converged to a torus and to a flock, when agents were started with random initial conditions, were calculated for increasing values of R_o and are shown in Figure 2.

3.2 Expressivity

Figure 2 shows the existence of what we term an *expressive region* in the parameter space, a set of parameters that allow multiple emergent behaviors. The existence of an expressive region affords switching between swarm behaviors simply by influencing a subset of the swarm. As can be seen in the figure, the expressive region is approximately $5 < R_o < 14$. Because it is desirable to have a flexible adaptable swarm that can express multiple behaviors we are interested in finding the model parameters that maximize expressivity.

We define the *expressive entropy* as a measure of the uncertainty of the emergent behavior of a swarm. In turn, the expressive entropy is a measure of how amenable the swarm is to switching its collective behavior given a large enough perturbation. Thus, expressive entropy tells us two things about a swarm: the sensitivity of the swarm to signals that

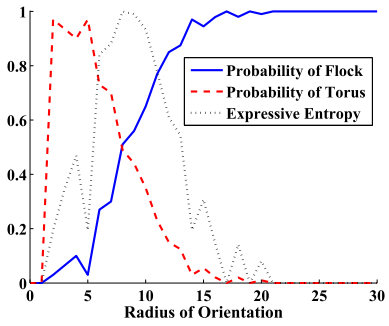

Figure 2: Probability of the swarm forming a flock or a torus as a function of the radius of orientation. The expressive entropy of the swarm is maximized at the point in the parameter space where a flock and torus are equally likely.

might make it change behavior and the uncertainty of what behavior will emerge.

The expressive entropy of a set of agents is defined as

$$H_{\text{exp}}(S_{\text{param}}) = \sum_{b \in Emergent[S_{\text{param}}]} p(b) \log_2 \left(\frac{1}{p(b)} \right) \quad (2)$$

where S_{param} denotes a specific point in the parameter space of the swarm model and $Emergent[S_{\text{param}}]$ is the set of emergent collective behaviors possible at S_{param}. For example, in Figure 2 all of the model parameters are fixed except for the radius of orientation so we are interested in the parameter subspace S_{param} for $0 < R_o < 30$. We also have $Emergent[S_{\text{param}}] = \{flock, torus\}$. Figure 2 shows H_{exp} as a function of the radius of orientation.

We see that $R_o \approx 8$ is the point in the parameter space with maximum expressive entropy, meaning that for agents that are randomly initiated within some constraints, both attractors are approximately equally probable. For this reason we use $R_o = 8$ for the remainder of this paper, but note that our results are robust to small deviations in this and other model parameters.[1]

We argue that this metric is relevant for the generalizablity of our approach because having the system operate at maximum expressive entropy induces an important tradeoff in the problem: maximum expressivity means that the system is as capable of switching between different collective states as possible which is good, but it also means that the estimation problem is harder because the prior probabilities of being in any given collective state are maximally uninformative—making it even more important that we can recognize the collective behavior of a swarm.

4. DETECTING COLLECTIVE BEHAVIOR

In this section we examine several global indicators of the collective behavior of a swarm and show how to classify these behaviors using local information from a small number of agents. We evaluate the performance of a very simple naive Bayes classifier and show that it achieves high accuracy while even in the presence of transients

4.1 Global indicators of collective behavior

Global indicators of collective behavior are important because they can be used to inform the selection of local agent-level features to approximate the collective behavior of a swarm. Additionally, as opposed to local features chosen in an ad hoc manner, features that are informed by global properties will most likely allow us to estimate the collective state effectively using limited samples.

Two different global measurements of collective behavior are often used to classify the emergent behavior of a swarm: group angular momentum, and group polarization [3, 6, 17]. Group angular momentum, m_{group}, is a measure of the degree of rotation of the group about the group centroid and is a value between 0 and 1. The group angular momentum of a swarm reaches a maximum value of 1 if all the agents rotate around the group centroid in the same direction. Group polarization, p_{group}, measures the degree of alignment among individuals within the group and is also a value between 0 and 1. The group polarization of a swarm reaches a maximum value of 1 when all the agents head in the same direction.

A torus is characterized by p_{group} close to 0 and m_{group} close to 1. A flock is characterized by p_{group} close to 1 and m_{group} close to 0. For the purpose of evaluating collective behavior recognition we subjectively define a swarm as a clockwise or counterclockwise torus if $m_{group} > 0.75$ $p_{group} < 0.25$ with the respective rotation. A swarm is defined as a flock if $m_{group} < 0.25$ and $p_{group} > 0.75$. These values yield classifications that are robust to minor perturbations, while ensuring the fundamental characteristics of a flock and torus are visually evident.

Examining the emergent behaviors in Figure 1 we see a clear spatial difference in the graph topology of the agents: agents are tightly packed in a flock, while a torus has a large void in the center. The underlying graph topology of a multi-agent system contains fundamental information about the global evolution of a group's behavior [9, 13] providing a strong theoretical foundation to our approach.

Based on these results we investigate a local approximation of the Fiedler eigenvalue of the underlying graph topology formed by agent interactions. The Fiedler eigenvalue, ν_{n-1}, is defined as the second smallest eigenvalue of the graph Laplacian and is a measure of the connectedness of the graph [4]. The underlying graph topology in multi-agent systems is known to be important for the convergence of consensus protocols and the speed of consensus is directly related to the algebraic connectivity or Fiedler eigenvalue [13]. The Laplacian L of an undirected graph is defined as $L = D - A$ where A is the adjacency matrix induced by the agent interactions and D is the diagonal matrix with agent degrees along the diagonal.

4.2 Local agent-level features

We have discussed three global features that distinguish between the flock and torus behaviors: group polarization, group momentum, and the Fiedler eigenvalue. We can use these global properties to motivate related local features.

The group polarization and momentum are related to agent headings and angular velocities, respectively. The Fiedler eigenvalue, ν_{n-1}, of a graph is related to the degree sequence

[1]Other parameters were set to $N = 100$, $s = 5$, $k = 0.5$, $R_o = 8$, and $R_r = 1$. Simulations used a discrete-time approximation with simulation time step of $\Delta T = 0.1$ seconds. Note that our results are robust to small deviations in this and other model parameters.

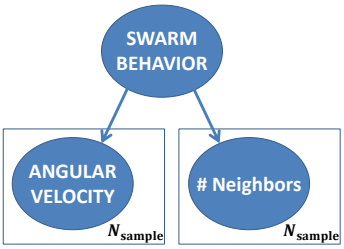

Figure 3: Bayesian network for swarm behavior classification using samples of local information from N_{sample} agents.

$(d_1, d_2, \ldots, d_n)$ of the graph by the relationship

$$0 \leq \nu_{n-1} \leq \frac{n}{n-1}\bar{d}, \tag{3}$$

where $\bar{d} = \frac{1}{n}\sum_i^n d_i$, and the degree of an agent is the number of neighbors it interacts with [4]. This relationship shows that ν_{n-1} is bounded above by the average degree, which can be estimated by local samples of agent degrees.

Thus, samples of individual agent angular velocities and numbers of neighbors (degrees) provide information to detect the group type of the swarm. Angular velocity from a few agents can be used to determine whether the agents are turning at approximately the same rate (torus) or moving straight (flock). The degree, or number of neighbors, of a few agents indicates whether the swarm's graph structure has high (flock) or low (torus) connectivity. These features do not require any kind of localization or shared frame of reference—they only require that an agent knows how fast it is turning and how many other agents are nearby.

4.3 Bayesian classification of swarm behavior

We make the Naive Bayes assumption that all features are conditionally independent given the collective behavior; see Figure 3. While this may not be true, success of this classifier provides evidence that using local estimates of a global indicator is a good approach— we don't need a sophisticated classifier to determine the collective state. This is important because when we operate at the point of maximum expressive entropy, the estimation problem is maximally hard in some sense. If a simple classifier can work, then it tells us that the global-to-local approach is sound.

Using the two local features discussed in Section 4.2, degree and angular velocity, we compute the Bayesian optimal estimate of the actual collective behavior, $\hat{b}_{\text{collective}}$ as follows

$$\hat{b}_{\text{collective}} = \underset{b}{\text{argmax}}\, P(b) \prod_{i \in \mathcal{S}} P\big(d_i \,\big|\, type\big) P\big(\omega_i \,\big|\, type\big) \tag{4}$$

where $b \in \{\text{clockwisetorus}, \text{counterclockwisetorus}, \text{flock}\}$, $\mathcal{S}$ is the set of agent samples, and d_i and ω_i are the degree and angular velocity obtained from the i^{th} agent sample, respectively. The individual likelihoods $P\big(d \,\big|\, type\big)$ and $P\big(\omega \,\big|\, type\big)$ are learned from training data. Because we are interested in collective behavior recognition at a point of maximum expressive entropy, we assume $P(torus) = P(flock) = 1/2$, although specific beliefs about the collective behavior of the swarm could be included.

4.4 Behavior classification data sets

To evaluate the accuracy of group type classification we created a training and a test set, both consisting of simulations for the flock and torus group types. Because a torus can form in one of two rotations, we attempt to recognize the rotation of the torus. The training data was obtained by initializing the swarm to form either a clockwise torus, counterclockwise torus, or flock. The test data was obtained by randomly initializing the swarm so it could form either a flock or a clockwise or counterclockwise torus.

4.4.1 *Training data*

To obtain data to model the numbers of neighbors and angular velocities of the flock and torus group types we ran three experiments: one for the flock, one for the clockwise torus, and one for the counterclockwise torus. Each experiment consisted of 100 replicates of 100 seconds each. For the flock simulations each agent's initial heading was set to $\theta = 0$ and the agents' starting locations were randomly chosen in the interval $[-20, 20] \times [-20, 20]$. These parameters were used because we found that they ensured that the swarm formed a flock. The initial positions for a torus were also chosen randomly, with initial headings set to $\theta_i = \text{atan2}(y_i, x_i) \pm \pi/2$, where the sign of $\pi/2$ was chosen depending on the desired orientation of the torus. This was done to ensure that the swarm formed a torus. For each simulation we let the group type stabilize for 25 seconds and then recorded the number of neighbors and angular velocity for each agent in the group every tenth of a second for the remainder of the simulation.

4.4.2 *Test data*

We created a test set by running 100 replicates with random initial headings and positions so that each simulation could produce either a flock or a torus. Out of the 100 simulations, 53 formed a torus and 47 formed a flock where the convergence was checked using the final m_{group} and p_{group} for each replicate. We also found that out of the 53 simulations that formed a torus, 26 formed a clockwise torus and 27 formed a counterclockwise torus.

4.4.3 *Estimating likelihoods*

We estimated the likelihood $P\big(d \,\big|\, type\big)$ of an agent having a certain number of neighbors d, given that the group is in a torus or a flock formation using the maximum likelihood estimate resulting from the training data.

To estimate the likelihood $P(\omega|type)$, we discretized angular velocity values using bins widths of .1 radians/second from -1.6 radians/second to 1.6 radians/second resulting in 32 bins then created a discrete probability distribution by binning all of the training data and normalizing the counts.

4.5 Classifying collective behavior

We let N_{sample} represent the number of agents sampled to obtain an estimate of the collective behaivor of the swarm. To simulate limited bandwidth we varied the number of agents sampled, N_{sample}, as well as the number successive samples taken from each of these agents. Samples were taken from agents every simulation update, corresponding to every 10th of a second. Because the test data is generated from simulations that started at random initial conditions, there can be a large amount of transient behavior before the group type stabilizes. To give ample time for a group type to form

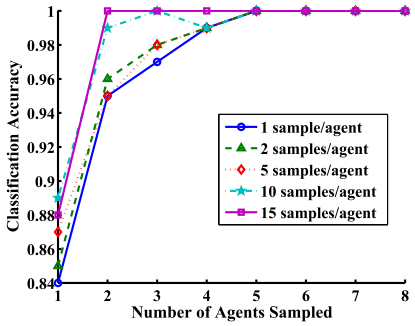

Figure 4: Collective behavior classification accuracy as the number of agents sampled increases for different numbers of successive samples per agent. Results are for a swarm with 100 agents.

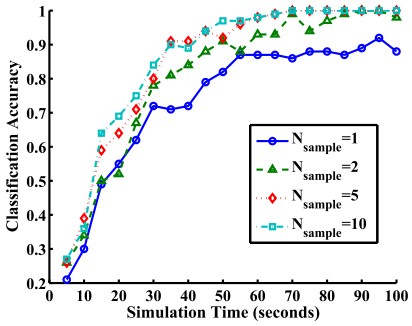

Figure 5: Accuracy for recognizing emerging collective behaviors despite transient dynamics. Results are for sampling once from N_{sample} different agents. By 100 seconds the collective behaviors have fully formed.

we gave the simulations 90 seconds to form and used the last 10 seconds (100 simulation updates) for computing the classification accuracy. This resulting classification accuracies are very high, as shown in Figure 4.

4.6 Effects of transients

Because it takes time for the collective behaviors to fully form, we investigated classifier performance in the presence of transient dynamics. To do this we evaluated the classification accuracy at 5 second intervals from 5 to 100 seconds of simulation time. We started sampling after 5 seconds of simulation time to mitigate the effects of initial positions and headings and to allow the group type to begin forming. This resulted in 20 different classification accuracies that we can compare to see how accuracy changes as the different group types emerge.

We used the number of neighbors and the angular velocity of sampled agents to classify between the clockwise torus, counterclockwise torus, and flock behaviors. Because of the transient behavior of the swarm at the beginning of the simulation we sampled only once from each agent every 5 seconds and classified the group behavior based only on the most recent samples taken.

The classification results for values of N_{sample} equal to 1, 2, 5 and 10 are shown in Figure 5. We see that the classifier performs extremely poorly when sampling once after only 5 seconds of simulation time. The reason for this is that many times an elongated flock-like transient forms and then flips into a torus. Also, simulations that actually formed flocks tend to start off very elongated, resulting in agents having fewer neighbors and the group type being initially classified as a torus. Thus, we conclude that while it is highly beneficial to wait for group types to form, group types can be classified with moderate accuracy early in the simulation while only sampling from a small percentage of the agents.

4.7 Discussion

We demonstrated that the collective behavior of a swarm can be accurately classified using samples from a small percentage of agents in a swarm. We showed that combining samples of the number of neighbors with samples of angular velocity achieves high classification accuracy. These results are robust to group types that are not fully formed, the inherent noise from our stochastic topology, and the precision loss that occurs when discretizing angular velocity.

While our results show extremely high accuracy, we note that this is because the flock and torus are stable distinct behaviors. This feature is desired in swarm behaviors because of the guaranteed robustness of the swarm to noise and agent errors. Thus, the robustness of the behaviors provides highly discriminative local agent-level features for easily recognizing the collective behavior of the swarm even when operating at a point of maximal expressiveness. The high accuracy achieved when sampling from only one agent also means that a single can classify the entire group behavior by itself. This is an important feature that could be applied to autonomous underwater or air vehicles that must cooperate with limited or no communication and which may change their behavior depending on what they perceive the entire collective is doing, without requiring message passing or convergence to a consensus.

We also demonstrated that the behavior of a swarm can be classified using samples of a few agents' number of neighbors and angular velocity. The classification was done using only features that did not require self localization or any kind of global reference frame. Because swarms may be tasked to environments where GPS is limited or unavailable and loss of communication or noisy signals may be common, monitoring a swarm in those scenarios is critical.

Before ending this section, note that we investigated the potential scalability of the classifiers for larger swarms. We calculated statistics for the number of neighbors and angular velocity of agents in a flock and torus of size $N = 200$, 300, and 400 and found that the distributions over an agent's number of neighbors and angular velocity continue to be distinct for larger group sizes. Table 1 shows the means and standard deviations for $N = 200$–400. Based on these results we hypothesize that accurate group type classification from limited samples is possible for larger groups. Future work should validate this hypothesis.

5. COUZIN'S MODEL

To demonstrate that the methods proposed for collective behavior recognition in Section 4 apply to other multi-agent systems, we consider Couzin's model [3]. Couzin's model [3] is similar to the Kerman swarm model, but has several

N	Behavior	#N μ	#N σ	AV μ	AV σ
200	Torus	19.20	4.14	0.38	0.25
	Flock	47.19	12.18	0.00	0.72
300	Torus	27.09	5.25	0.37	0.32
	Flock	62.39	15.89	0.00	0.74
400	Torus	34.39	6.28	0.36	0.37
	Flock	75.98	19.06	0.00	0.75

Table 1: The sample means (μ) and standard deviations (σ) for the distributions of number of neighbors (#N) and angular velocity (AV) as the size of the swarm, N, increases.

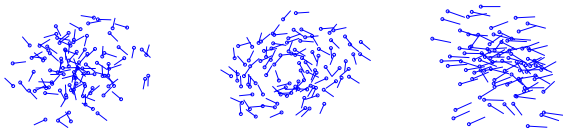

(a) swarm (b) torus (c) flock

Figure 6: Emergent behaviors in Couzin's model. Straight lines represent agent headings.

key differences: (1) it produces three distinct group types: a swarm, a torus, and a flock (see Figure 6), (2) agents have a blind spot, (3) it uses a fixed maximum turning rate instead of using integrator dynamics, (4) it uses non-stochastic and non-overlapping behavior zones to create a metric topology with a maximum sensing range R_a, and (5) it adds explicit noise to the individual agent headings.

The agent dynamics in Couzin's model are similar to Kerman's model; agents repel from neighbors within a repulsion radius R_r, orient with agents within an orientation zone R_o, and attract to agents within an attraction zone R_a. The model consists of N agents that move at a constant speed s, have a vision range of α radians, and can turn at most β radians per second. Agents update their heading and position every Δt seconds.[2]

5.1 Expressive regions

To find parameter settings that can exhibit multiple group types, we performed an experiment similar to the one discussed in previously, but for Couzin's model. We ran a series of 100 replicates for values of R_o between 1 and 10 in 0.5 unit increments. We then used the results of the final state of the simulation after 100 seconds to determine what group type had formed. Each replicate was started from random initial conditions. We determined the ground truth behavior as follows

$$b_{\text{collective}} = \begin{cases} \text{swarm}, & \text{if } m_{group} < 0.3 \text{ and } p_{group} < 0.3 \\ \text{torus}, & \text{if } m_{group} > 0.6 \text{ and } p_{group} < 0.3 \\ \text{flock}, & \text{if } m_{group} < 0.3 \text{ and } p_{group} > 0.6 \end{cases} \quad (5)$$

where the torus behavior was designated as either a clockwise or counterclockwise torus based on the rotational direction of the majority of the agents in the swarm. Because the group types in Couzin's model do not form as clearly as in Kerman's model, these conditions are more relaxed.

[2]Simulation parameters were $N = 100$, $R_r = 1$, $R_a = 15$, $s = 3$ units/second, $\alpha = 5\pi/3$ radians, and $\beta = 1.4$ radians, and $\Delta t = 0.1$ seconds. We added $\eta \in \mathcal{U}(-0.2, 0.2)$ radians/second of noise to the individual agent headings, where $\mathcal{U}(\cdot, \cdot)$ is the continuous uniform distribution.

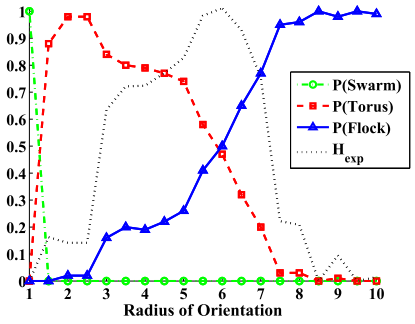

Figure 7: Probability of Couzin's model producing either a swarm, a torus, or a flock for different values of R_o. The expressive entropy H_{exp} is maximized at the point where a flock and a torus are approximately equally likely.

Figure 7 shows the probability of each group type forming for each value of R_o that was simulated. We see that there is not an expressive region that forms both swarm and torus behaviors. This is because once the radius of orientation is greater than the radius of repulsion, the agents start orienting with each other and the swarm undergoes a phase transition and forms a torus. This can be seen by the immediate jump in the probability of forming a torus and the immediate drop in the probability of forming a swarm when R_o is increased from 1 to 1.5. As the radius of orientation is increased past 1.5, the torus stabilizes and then, for high enough values of R_o, flocks become the dominant group type. Figure 7 also shows the expressive entropy of the swarm. We use $R_o = 6$ as the point in the parameter space that approximately maximizes expressive entropy.

We examined the simulations that didn't meet any of the criteria in Equation 5 and found that they either formed a noisy torus with agents rotating in the both directions (for $R_o = 1.5$) or formed something in between a flock and a torus, with most of the agents clumped up but still moving around in circles. We also checked for fragmentation by looking at the positions of the agents at the end of each the simulation and checking to see if the underlying interaction graph formed by the radius of attraction was connected. We found that only two of the simulations fragmented. These two simulations were not used in the following analysis.

5.2 Classification features

We used the same features used in Section 4. We calculated the distributions over number of neighbors and angular velocity for a swarm, a torus, and a flock using the same simulations used to investigate the expressive region in Couzin's model. We used the 100 replicates with $R_o = 1$, the 98 replicates that formed a clockwise or counterclockwise torus when $R_o = 2$, and the 99 replicates that formed a flock and did not fragment when $R_o = 8.5$ to model the swarm, clockwise and counterclockwise torus, and flock, respectively. The torus rotation was determined by inspecting the final angular velocity of each agent for each replicate. We

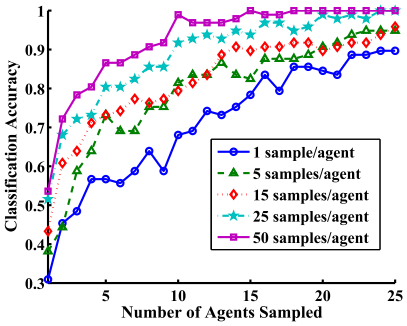

Figure 8: Behavior recognition accuracy for distinguishing between a flock, a clockwise torus, and a counterclockwise torus in Couzin's swarm model.

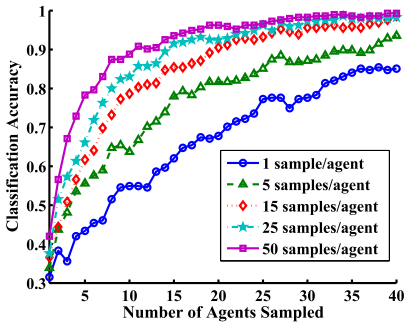

Figure 9: Behavior recognition accuracy for distinguishing between a swarm, a clockwise torus, a counterclockwise torus, and a flock in Couzin's swarm model.

found that there were 47 clockwise torus simulations, and 51 counterclockwise torus simulations.

Figure 6 shows a snap shot of a swarm, torus, and flock. Because all three group types tend to be tightly packed with the torus lacking the large void that is found in Kerman's model, the distributions of numbers of neighbors and angular velocities in Couzin's model are similar making it harder to detect the collective behavior of the swarm.

5.3 Torus and flock classification

Because there is no expressive region that allows both a swarm and a torus to form, we first investigate only discriminating between the torus and flock group types. We created a test set of 100 simulations using $R_o = 6$ to test the accuracy of a naive Bayes classifier using the number of neighbors and angular velocity as features. Using $R_o = 6$ will form either a flock or a torus with approximately equal probability. Thus, there are three possible classifications: a clockwise torus, a counterclockwise torus, or a flock. Figure 8 shows how the classification accuracy changes as the bandwidth constraint on the number of agents sampled and the number of successive samples take from each agent changes.

The classification accuracies for Couzin's model are much lower than for Kerman's model (see Figure 4), but we see that sampling more than 10 agents provides high classification accuracies as long as a sufficient number of samples are taken. The lower classification accuracies were a result of most of the flock simulations being misclassified as either a clockwise or counterclockwise torus. Increasing the bandwidth and number of samples increases the accuracy, but the majority of the errors still come from misclassifying a flock as a torus. When $N_{\text{sample}} \geq 5$ and at least 5 samples/agent are used, there are no misclassifications between the clockwise and counterclockwise torus. Thus, our chosen features discriminate well between torus behaviors, but do not discriminate as well between a flock and a torus.

5.4 Swarm, torus, and flock classification

Couzin's model has an expressive region where both the torus and flock behaviors can form, but has a phase transition between the swarm and torus behaviors. Because of this there is no single set of parameters that will form either a swarm or torus with equal probability. However, it is still interesting to see if group type classification can be done with high accuracy when the swarm can be in more than three behaviors. To test the classification accuracy in this case, we created a test set with 100 simulations of a swarm ($R_o = 1$), 100 simulations of a torus ($R_o = 2$), and 100 simulations of a flock ($R_o = 8.5$). This simulates a point of maximum expressivity, because each behavior (swarm, torus, and flock) has a 1/3 chance of emerging. The values of R_o were chosen to ensure a high likelihood of every simulation forming the desired group type. All other parameters were kept the same as before, and each simulation was started with random initial positions and headings.

Before computing the accuracy of the classifier we checked each simulation's final m_{group} and p_{group} to see if the desired group type had formed. We also checked the final positions of the agents to check for group fragmentation. We found that none of the simulations fragmented for any of the parameter settings. For $R_o = 1$, all 100 of the simulations formed a swarm. For $R_o = 2$, 93 of the simulations formed a torus, 4 simulations formed a flock, and 3 simulations failed to converge to a distinct group type. For $R_o = 8.5$, 98 of the simulations formed a flock and 2 never formed a distinct group type. In the subsequent analysis we use only the simulations that fully formed a group type. This resulted in a test set of 295 simulations.

Figure 9 shows classification accuracy as a function of N_{sample}. The classification accuracies with three group types are noticeably lower than with two possible group types. As before, using more samples increases accuracy, and that more samples are needed to reach high classification accuracies with Couzin's model than for classification using Kerman's model. We examined the classification errors and found that most of the errors came from from misclassifying a behavior as a swarm or misclassifying a swarm as another behavior. We also found that the largest number of these errors occur between the flock and swarm group types. This was found to be a result of the similarity between the distributions for the number of neighbors and angular velocity of a flock and of a swarm. This is a case where adding information about agent headings would be beneficial.

6. SUMMARY AND FUTURE WORK

This research focuses on a major problem that impedes scalable interactions with large bio-inspired robot swarms: accurately detecting the collective state of a robot swarm using limited information from a subset of the swarm. We

presented a formal metric called expressive entropy that can be used to determine the point in the parameter space with maximum expressivity. We propose that swarm systems should operate at, or near, the point of maximum expressive entropy to provide the maximum flexibility in possible collective behaviors. However, maximizing the expressive entropy of a swarm also means that the estimation problem is harder because the prior probabilities of being in any given collective state are maximally uninformative.

We presented a novel framework for classifying the collective behavior of a bio-inspired robot swarm using locally-based approximations of global features of the emergent collective behaviors. Using a bio-inspired model of swarming proposed by Kerman et al. [6], we showed that even if agents are not capable of determining their location or heading, we can accurately classify the group behavior of the swarm using local samples from individual agents. This accuracy remains high even if limited bandwidth restricts the number of observable agents. We investigated behavior recognition for swarms undergoing transient dynamics and provided evidence that our method of detecting collective behavior from limited samples scales to larger swarm sizes.

We also demonstrated that our methodology for behavior recognition generalizes to Couzin's swarm model [3]. Kerman's model has collective behaviors that are very distinct and afford high accuracy behavior recognition with very low bandwidth. Couzin's model, on the other hand, has emergent behaviors that are not as distinct which resulted in lower accuracies and higher bandwidth requirements to sample more agents. Thus, while we hypothesize that our approach is applicable to many other multi-agent systems, depending on the distinctness of the collective behaviors, obtaining high recognition accuracy with limited bandwidth may require sampling agent positions and headings and using more complex models such as Hidden Markov Models or Conditional Random Fields [20].

Future work should investigate how well the methods we described scale to larger swarm sizes and also investigate how human or environmental influences affect behavior recognition accuracy. Other future work includes applying our collective behavior recognition framework to more complex swarm behaviors, to models with many emergent behaviors, and to actual robot swarms.

7. REFERENCES

[1] N. Bode, D. Franks, and A. Wood. Limited interactions in flocks: relating model simulations to empirical data. *Journal of The Royal Society Interface*, 8(55):301–304, 2010.

[2] D. S. Brown. Toward scalable human interaction with bio-inspired robot teams. Master's thesis, Brigham Young University, Provo, UT, 2013.

[3] I. Couzin, J. Krause, R. James, G. Ruxton, and N. Franks. Collective memory and spatial sorting in animal groups. *Journal of Theoretical Biology*, 218(1):1–11, 2002.

[4] D. Cvetkovic, P. Rowlinson, and S. Simic. *An introduction to the theory of graph spectra*. Cambridge University Press, 2010.

[5] L. E. Dubins. On curves of minimal length with a constraint on average curvature, and with prescribed initial and terminal positions and tangents. *American J. of Mathematics*, vol. 79, no. 3, 1957.

[6] S. Kerman, D. Brown, and M. Goodrich. Supporting human interaction with robust robot swarms. In *Proceedings of the International Symposium on Resilient Control Systems*, Aug 2012.

[7] H. Levine, W. Rappel, and I. Cohen. Self-organization in systems of self-propelled particles. *Physical Review E*, 63(1):017101, 2000.

[8] J. Marshall, M. Broucke, and B. Francis. Formations of vehicles in cyclic pursuit. *IEEE Transactions on Automatic Control*, 49(11):1963–1974, 2004.

[9] M. Mesbahi and M. Egerstedt. *Graph Theoretic Methods in Multiagent Networks*. Princeton University Press, 2010.

[10] A. L. Nevai, K. M. Passino, and P. Srinivasan. Stability of choice in the honey bee nest-site selection processs. *Journal of Theoretical Biology*, 263(1):93–107, 2010.

[11] M. Novitzky, C. Pippin, T. R. Collins, T. R. Balch, and M. E. West. Bio-inspired multi-robot communication through behavior recognition. In *2012 IEEE International Conference on Robotics and Biomimetics (ROBIO)*, pages 771–776. IEEE, 2012.

[12] R. Olfati-Saber. Flocking for multi-agent dynamic systems: Algorithms and theory. *IEEE Transactions on Automatic Control*, 51(3):401–420, 2006.

[13] R. Olfati-Saber, J. Fax, and R. Murray. Consensus and cooperation in networked multi-agent systems. *Proceedings of the IEEE*, 95(1):215–233, 2007.

[14] J. Patrix, A.-I. Mouaddib, S. Le Gloannec, D. Stampouli, and M. Contat. Discrete relative states to learn and recognize goals-based behaviors of groups. In *Proceedings of the 12th International Conference on Autonomous Agents and Multiagent Systems*, pages 933–940. International Foundation for Autonomous Agents and Multiagent Systems, 2013.

[15] C. Reynolds. Flocks, herds and schools: A distributed behavioral model. In *ACM SIGGRAPH Computer Graphics*, volume 21, pages 25–34. ACM, 1987.

[16] E. Şahin. Swarm robotics: From sources to domains of application. In *Swarm Robotics*, pages 10–20. Springer, 2005.

[17] D. Strömbom. Collective motion from local attraction. *Journal of Theoretical Biology*, 283(1):145–151, 2011.

[18] G. Sukthankar and K. Sycara. Robust recognition of physical team behaviors using spatio-temporal models. In *Proceedings of the Fifth International Joint Conference on Autonomous Agents and Multiagent Systems*, pages 638–645. ACM, 2006.

[19] D. J. Sumpter. *Collective animal behavior*. Princeton University Press, 2010.

[20] D. L. Vail, M. M. Veloso, and J. D. Lafferty. Conditional random fields for activity recognition. In *Proceedings of the 6th International Joint Conference on Autonomous Agents and Multiagent Systems*, page 235. ACM, 2007.

[21] T. Vicsek, A. Czirók, E. Ben-Jacob, I. Cohen, and O. Shochet. Novel type of phase transition in a system of self-driven particles. *Physical Review Letters*, 75(6):1226–1229, 1995.

[22] T. Vicsek and A. Zafeiris. Collective motion. *Physics Reports*, 517(3):71–140, 2012.